Journal of the Korean Nuclear Society
Volume 32, Number 5, pp.433~445, October, 2000

Development of the Interfacial Area Concentration Measurement Method Using a Five Sensor Conductivity Probe

Dong-Jin Euh, Byong-Jo Yun, Chul-Hwa Song, Tae-Soon Kwon, and Moon-Ki Chung
Korea Atomic Energy Research Institute
150 Dukjin-dong, Yusong-gu Taejon 305-353, Korea
djeuh@kaeri.re.kr

Un-Chul Lee
Seoul National University
San 56-1 Shinrim-dong, Gwanak-gu, Seoul, 151-742, Korea

(Received October 29, 1999)

Abstract

The interfacial area concentration (IAC) is one of the most important parameters in the two-fluid model for two-phase flow analysis. The IAC can be measured by a local conductivity probe method that uses the difference of conductivity between water and air/steam. The number of sensors in the conductivity probe may be differently chosen by considering the flow regime of two-phase flow. The four sensor conductivity probe method predicts the IAC without any assumptions of the bubble shape. The local IAC can be obtained by measuring the three dimensional velocity vector elements at the measuring point, and the directional cosines of the sensors. The five sensor conductivity probe method proposed in this study is based on the four sensor probe method. With the five sensor probe, the local IAC for a given referred measuring area of the probe can be predicted more exactly than the four sensor probe. In this paper, the mathematical approach of the five sensor probe method for measuring the IAC is described, and a numerical simulation is carried out for ideal cap bubbles of which the sizes and locations are determined by a random number generator.

Key Words : five sensor conductivity probe, two-phase flow, cap bubble, interfacial area concentration (IAC)

1. Introduction

The interfacial area concentration (IAC), which is defined as the interface area per unit control volume, is one of the most important parameters in the two-fluid model for a two-phase flow

analysis. The conductivity probe method is a useful measurement technique for flow parameters, such as the void fraction and bubble velocity in two-phase flow. It uses the difference of conductivity between water and air/steam. The measuring principle of the multi-sensor conductivity probe in obtaining a local time-averaged IAC is based on the mathematical formulation given by Ishii[1] as follows:

$$\bar{a}_i^t(x_0,y_0,z_0)=\frac{1}{\Omega}\sum_j\frac{1}{|\vec{v}_{ij}|\cos\phi_j} \quad (1)$$

The IAC can be obtained by measuring the interface velocity and number frequency of the interfaces at a local measuring point.

The number of sensors included in a conductivity probe is usually two or four, and their applicability depends on the flow regimes or particle shape. The double probe method uses the assumptions that there is no correlation between the interface velocity vector and surface normal vector and that the particle shape is spherical. Therefore the double probe method is applicable only to the bubbly flow.[2-7] The four sensor probe consists of one central common sensor and three rear sensors. The four sensor probe method does not require any statistical assumptions.[8-10] The concept of the five sensor probe method proposed in this study is similar to that of the four sensor probe method. It can measure the IAC more systematically by obtaining an additional axial velocity vector from the central rear sensor than four sensor probe.

In this study, the theoretical approach for the local IAC measuring method using a five sensor conductivity probe is presented, and its validity is shown by a numerical simulation for ideal cap bubbles of which the sizes and locations are determined by a random number generator.

2. Theory

2.1. Four Sensor Probe Method [8-10]

If a function representing a moving gas-liquid interface, j, is defined as Eq. (2), the local instantaneous IAC is given in terms of the distribution as shown in Eq. (3):

$$f_j(x,y,z)=0 \quad (2)$$

$$\bar{a}_i(x,y,z,t)=\sum_j|\nabla f_j|\,\delta f_j(x,y,z,t) \quad (3)$$

This formulation is valid for any flow regime of the two-phase flow. Since the distribution, $\delta f_j(x,y,z,t)$, is not experimentally observable, the time-averaged value of the IAC is usually used. In time duration Ω at a local position (x_0,y_0,z_0,t_0), the local IAC is given by

$$\bar{a}_i^t(x_0,y_0,z_0)=\frac{1}{\Omega}\sum_j\left\{|\vec{\nabla}f_j|/\left|\frac{\delta f_j}{\delta t}\right|\right\}_{at(x_0,\,y_0,\,z_0)} \quad (4)$$

Referring to Fig. 1, the following relation can be obtained.

$$|\vec{\nabla}f_j|/\left|\frac{\delta f_j}{\delta t}\right|=\frac{1}{|\vec{v}_{ij}|\cos\phi_j} \quad (5)$$

From Eqs. (4) and (5), the time-averaged IAC can be derived as follows:

$$\bar{a}_i^t(x_0,y_0,z_0)=\frac{1}{\Omega}\sum_j\frac{1}{|\vec{v}_{ij}|\cos\phi_j} \quad (6)$$

where ϕ_j is the angle between the velocity of the j-th interface, $\vec{v}_{ij}$, and the direction of the surface normal vector at , as shown in Fig. 1.

For a sufficiently large time duration, Ω, one obtains the following relation,

$$\left(\sum_j\right)=\Omega/\tau \quad (7)$$

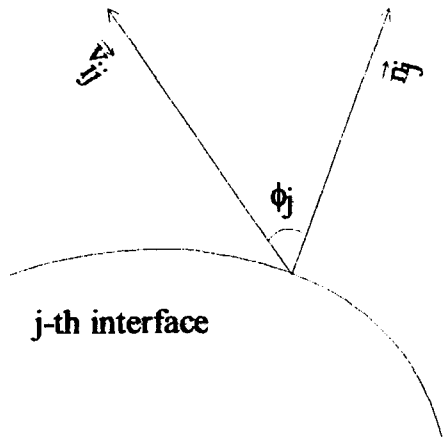

Fig. 1. Angle Between $\vec{v}_{ij}$ and $\vec{n}_j$

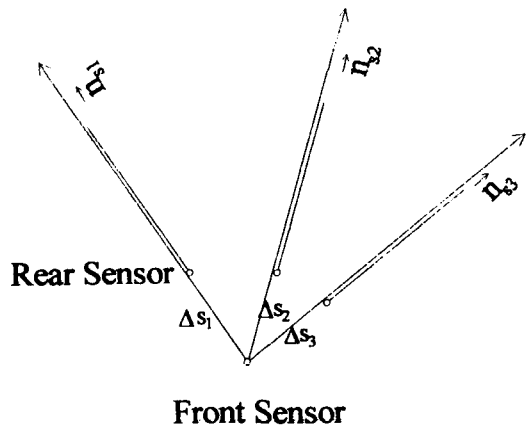

Fig. 2. Schematic of Four Sensor Probe

where τ can be expressed by $\tau=1/(2N_t)$ if one defines N_t as the particle number passing the measuring point per unit time. Substituting Eq. (7) into Eq. (6), one can get the following formula of the IAC:

$$\bar{a}_i^t(x_0,y_0,z_0)=\frac{1}{\tau}\overline{\frac{1}{|\vec{v}_{ij}|\cos\phi_j}} \tag{8}$$

Fig. 2 shows a schematic of the four sensor probe. The unit vector, $\vec{n}_{sk}$, for a rear sensor, k, is represented by $(\cos\eta_{xk}, \cos\eta_{yk}, \cos\eta_{zk})$, with k=1,2,3. The location of the front sensor is given by (x_0, y_0, z_0) and that of the rear sensor, k, by (x_k, y_k, z_k) . The velocity of j-th interface passing the rear sensor, k, through the front sensor with a time interval, Δt_{kj}, can be defined by

$$v_{ikj}=\frac{\Delta s_k}{\Delta t_{kj}}, \qquad k=1,2,3 \tag{9}$$

If the j-th interface is expressed by $f_j(x,y,z,t)$, then the following relations are satisfied.

$$f_j(x_0,y_0,z_0,t_j)=0 \tag{10}$$

$$f_j(x_k,y_k,z_k,t_j+\Delta t_{kj})=0 \tag{11}$$

Assuming the distance, Δs_k, and the time difference, Δt_{kj}, are sufficiently small compared to the length and time scales, respectively, the following relation can be obtained from Eqs. (10) and (11)

$$\frac{\partial f_j}{\partial x}\cos\eta_{xk}+\frac{\partial f_j}{\partial y}\cos\eta_{yk}+\frac{\partial f_j}{\partial z}\cos\eta_{zk}=-\frac{\partial f_j}{\partial t}\frac{1}{v_{ikj}} \tag{12}$$

If the unit vectors, $\vec{n}_{s1}$, $\vec{n}_{s2}$, $\vec{n}_{s3}$, are linearly independent, then the determinant $|A_0|$ is as follows:

$$|A_0|=\begin{vmatrix}\cos\eta_{x1} & \cos\eta_{y1} & \cos\eta_{z1}\\ \cos\eta_{x2} & \cos\eta_{y2} & \cos\eta_{z2}\\ \cos\eta_{x3} & \cos\eta_{y3} & \cos\eta_{z3}\end{vmatrix}\neq 0 \tag{13}$$

Then, the solution of Eq. (12) is expressed by

$$(|\vec{v}_{ij}|\cos\phi_j)^{-1}=\frac{\sqrt{|A_1|^2+|A_2|^2+|A_3|^2}}{\sqrt{|A_0|^2}} \tag{14}$$

where the determinants $|A_1|$, $|A_2|$, $|A_3|$ are given by

$$|A_1| = \begin{vmatrix} \frac{1}{v_{i1j}} & \cos\eta_{y1} & \cos\eta_{z1} \\ \frac{1}{v_{i2j}} & \cos\eta_{y2} & \cos\eta_{z2} \\ \frac{1}{v_{i3j}} & \cos\eta_{y3} & \cos\eta_{z3} \end{vmatrix}, \quad (15)$$

$$|A_2| = \begin{vmatrix} \cos\eta_{x1} & \frac{1}{v_{i1j}} & \cos\eta_{z1} \\ \cos\eta_{x2} & \frac{1}{v_{i2j}} & \cos\eta_{z2} \\ \cos\eta_{x3} & \frac{1}{v_{i3j}} & \cos\eta_{z3} \end{vmatrix}, \quad (16)$$

$$|A_3| = \begin{vmatrix} \cos\eta_{x1} & \cos\eta_{y1} & \frac{1}{v_{i1j}} \\ \cos\eta_{x2} & \cos\eta_{y2} & \frac{1}{v_{i2j}} \\ \cos\eta_{x3} & \cos\eta_{y3} & \frac{1}{v_{i3j}} \end{vmatrix} \quad (17)$$

Finally, the time-averaged IAC is given by

$$\bar{a}_i^t = \frac{1}{\Omega}\sum_j \frac{\sqrt{|A_1|^2 + |A_2|^2 + |A_3|^2}}{\sqrt{|A_0|^2}} \quad (18)$$

Thus, the local time-averaged IAC can be obtained by measuring the three-dimensional interfacial velocity components at a measuring point, and the geometric parameters of the four sensor probe.

This equation can be applied only to the case that an interface passes all of the tips of the four sensors. However, because of the finite size of the probe, some interfaces passing the front sensor may not hit one of the rear sensors. When the probe is positioned near the wall, the trend is significant. The contribution of the interfacial area from such missing interfaces would be substantial and must be considered. For such missing interfaces, the IAC is obtained by following mathematical formula under the assumption that

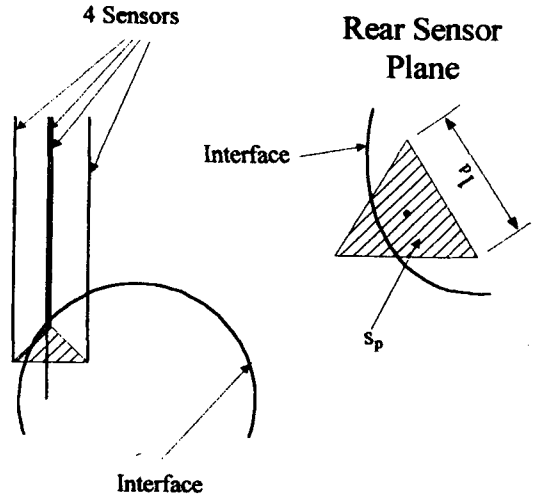

Fig. 3. Configuation of the Missing Interface

the shape of the interface is steep, and nearly parallel to the probe:

$$a_{ij} = \frac{\tau_b}{\Omega}\frac{l_d}{s_p} \quad (19)$$

In this formula, l_d is the distance between two of the rear sensors, s_p is the projected area of the probe in the flow direction as shown in Fig. 3, and τ_b is the bubble residence time.

2.2. Five Sensor Probe Method

A design of a typical five sensor probe is shown in Fig. 4. The probe includes a central front sensor, a central rear sensor, and three peripheral rear sensors. The measuring point is the location of the central front sensor. From the central rear sensor, one can additionally obtain the axial velocity component of the interface. Thus the four velocity components of the interface at a measuring point can be obtained, and the IAC can then be determined from the three sub-cells in the measuring area independently as shown in Fig. 5. The direction vector components of the rear

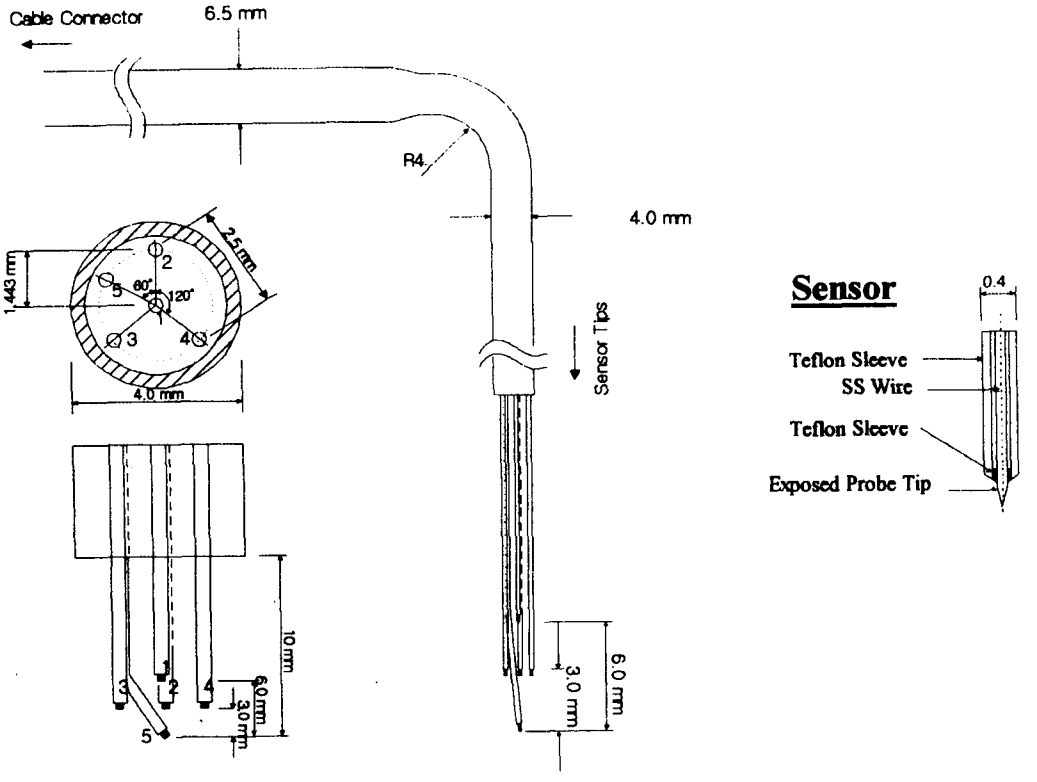

Fig. 4. Prototype of the Five Sensor Conductivity Probe

sensors from the central front sensor are derived from the consideration of the geometry of the probe. The derivation of the directional vector components is described in appendix A.

Generally, the interface is not symmetrical on the central sensor, and the IAC at the central measuring point would then be different according to the referred sub-cell. The IAC is obtained by weighted averaging for the angle of each sub-cell on the measuring point. This process has some advantages such that the curvature effect of interface can be reduced for a given size of the probe, and that a more systematic approach for missing bubbles can be made when compared with the four sensor probe method. Most of the missing interfaces usually have steep shapes and the IAC for those interfaces at the measuring point would be estimated as large. Thus the contribution of the interfacial area from the missing interfaces cannot be neglected.

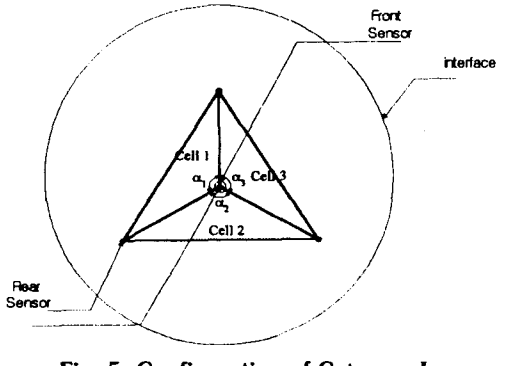

Fig. 5. Configuration of Category I

In this study, several types of interfaces passing through the sensors are classified into four categories, and different mathematical formulations are applied to each category. The configuration formed by the sensor tips and the

projected bubble interface is shown in Figs. 5~9 for each category.

2.2.1. Category I (Case 1) : For Interfaces Passing all of the Rear Sensors

In this case, three triangle shaped sub-cells can be considered on the central position, as shown in Fig. 5. The three-dimensional interfacial velocity vector can be obtained from each cell independently at a local measuring point. Thus, three values of the IAC at the central measuring point can be made. The IAC representing the quantity at the measuring point is obtained by weighted averaging for the angle defined in Fig. 5 as follows:

$$a_{ij} = \frac{(a_{ij})_{Cell\,1}\alpha_1 + (a_{ij})_{Cell\,2}\alpha_2 + (a_{ij})_{Cell\,3}\alpha_3}{2\pi} \quad (20)$$

The IAC for each sub-cell k, $(a_{ij})_{cell\ k}$, is obtained from the four sensor probe method. This method has the advantage that the curvature effect of the interface can be reduced for a given size of the probe.

2.2.2. Category II (Case 2~4) : For Interfaces Passing Two Sensors among the Three Symmetrical Rear Sensors

This category is also divided into three cases according to the kind of the missing sensor among the three symmetrical rear sensors, and the same methodology can be applied to the three cases. Similar to category I, the IAC is obtained from the weighted averaging process as in Eq. (20) by considering the three sub-cells. Fig. 6 shows the configuration and projected triangle of one of the three cases. The IAC of sub-cell 1 is obtained by the four sensor probe method, but since all of the three components of the velocity vector cannot be measured in the other sub-cells, some mathematical considerations, which are somewhat different from the four sensor method, are made in this category. A sensor detects two interfaces per bubble, and one can expect that the upper side of the missing interface is steep, but the bottom is flat, unless the bubble is small. The steepness of an interface can be judged by comparing the value referring to cell 1 with the value of a flat interface (Inequality in Eq. (21)). For the steep interface, the interface is assumed to be nearly parallel to the probe. For a flat type of interface, the value referring to cell 1 can be considered as the representing value on the

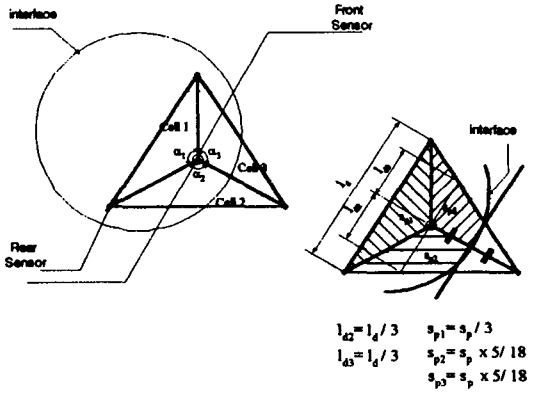

Fig. 6. Configuration of Category II

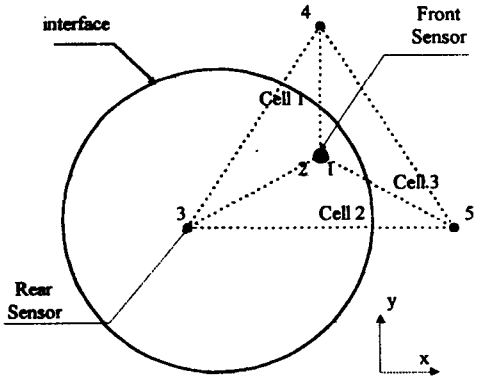

Fig. 7. Configuration of Category III

measuring point. For any other shape of the interface, some mathematical considerations are applied in cell 2, 3, as shown in Eq. (21).

In this study, the criteria of a 5% difference is used. This relation, Eq. (21), can be applied to any interface having various steepnesses. l_{dk} and s_{pk} are the length and area that is occupied by a bubble in the cell k, and they are determined by using some statistical assumptions that the bubble occupies the projected area as in Fig. 6. When the projected area is divided equally into the three sub-cells, the length and area in the sub-cells are also given in Fig. 6.

$$\begin{aligned}
&\text{for } \left|\left(a_{ij}\right)_{\text{Cell 1}} - \frac{1}{\Omega}\frac{1}{v_{iz}}\right| < \varepsilon \\
&\quad \left(a_{ij}\right) = \left(a_{ij}\right)_{\text{Cell 1}} \\
&\text{for } \left|\left(a_{ij}\right)_{\text{Cell 1}} - \frac{1}{\Omega}\frac{1}{v_{iz}}\right| > \varepsilon \\
&\quad \left(a_{ij}\right)_{\text{Cell 2}} = \frac{\tau_b\, l_{d2}}{\Omega\, s_{p2}} \\
&\quad \left(a_{ij}\right)_{\text{Cell 3}} = \frac{\tau_b\, l_{d3}}{\Omega\, s_{p3}}
\end{aligned} \tag{21}$$

2.2.3. Category III (Case 5~7) : For Interfaces Passing One Sensor among the Three Symmetrical Rear Sensors

This category is also divided into three cases according to the missing sensor among the three symmetrical rear sensors, and a methodology can be applied for each case. For these cases, some mathematical considerations are made because only two components of the velocity vector for each cell can be obtained. Fig. 7 shows one of the three cases belonging to this category. For this case, an exact relation (see Eq. (27)) is considered to have the IAC. The x or y directional slope cannot be measured directly at the local measuring point, 1, so some engineering considerations based on the measurable quantities are made.

Let us consider a case that an interface contacts the sensors, 1, 2, and 3. Because one can statistically expect that the slopes of the interface in the direction of x and y at the measuring point, 1, would be larger than the linear slopes in each direction between the sensors, 1 and 3, the elevation difference of the interface in each direction is assumed to be that at the position of the sensors, 1 and 3. The IAC is then derived by

$$\left(a_{ij}\right) = \frac{1}{\Omega}\frac{1}{v_{iz}}\sqrt{1+\left(\frac{\Delta z_{13}}{\Delta x_{13}}\right)^2+\left(\frac{\Delta z_{13}}{\Delta y_{13}}\right)^2} \tag{22}$$

The lengths in the denominators of the terms in root, Δx_{13} and Δy_{13}, are the distance between sensors 1 and 3 in the x and y direction, respectively, and are determined by the geometry of the probe. The elevation difference of the surface at sensors 1 and 3, Δz_{13}, is obtained from the axial velocity component and the delay time of the rear sensor signal. Subscripts 1 and 3 are the identification numbers of the sensors. If Δx_{13} or Δy_{13} is 0, the slope of the interface in the direction of either axis is hard to be obtained. For the case, the measuring point is assumed to be at the location shown in Fig. 8.

2.2.4. Category IV (Case 8) : For Interfaces Passing Only the Two Central Sensors

Under the assumption that the bubbles have a spherical shape, the double sensor probe method presented by Revankar et al.[3], and Hibiki et al.[7] can be applied as follows:

$$a_{ij} = \frac{2\frac{1}{|v_{iz}|}}{\Omega\left(1-\cot\frac{\alpha_0}{2}\ln\left(\cos\frac{\alpha_0}{2}\right)-\tan\frac{\alpha_0}{2}\ln\left(\sin\frac{\alpha_0}{2}\right)\right)} \tag{23}$$

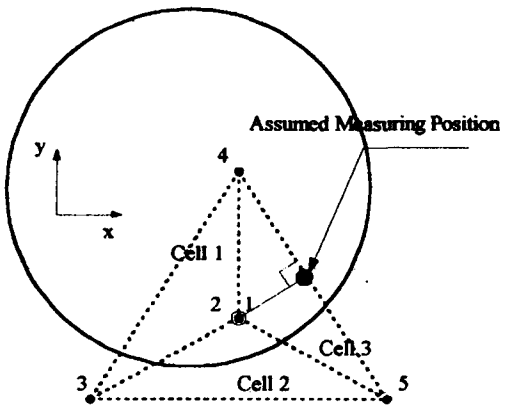

Fig. 8. Case 5, Modifed

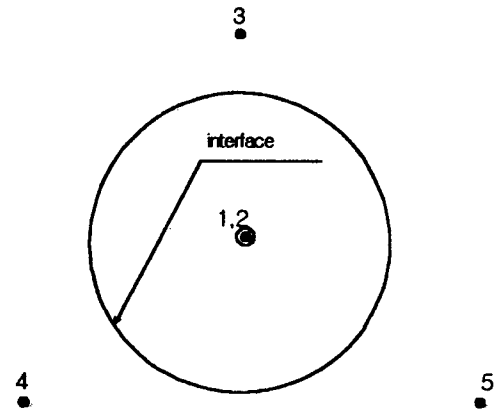

Fig. 9. Configuration of Category IV

If the variables related to the velocity fluctuation, α_0(see nomenclature) is assumed to be nearly 0, then Eq. (23) is simplified to Eq. (24).

$$a_{ij} = \frac{2}{\Omega} \frac{1}{|v_{iz}|} \tag{24}$$

This equation is applied to the numerical simulation presented in the following section. Since the contribution of the IAC from the interfaces of the case 8 is small, as will be presented later, this simplification is valid.

2.2.5. Total Time-Averaged IAC

The total time-averaged IAC is obtained by the summation of the instantaneous values for the interfaces of various cases as follows:

$$\bar{a}_i^t = \sum_j a_{ij} \tag{25}$$

3. Numerical Simulation for Artificial Cap Bubbles

To verify the applicability of the five sensor probe method, a numerical simulation is performed. The flow channel is assumed to be cylindrical and to have a 0.08m ID. The geometry of the five sensor probe applied in this test is shown in Fig. 4. The generated bubbles were assumed to have cap shape. The size of a bubble is determined by using a random number generated from the random number generator, and the generated location in the channel is by two additional random numbers. The generated bubbles are assumed to have the exponential size distribution of Nukiyama et al.[11] By considering 20 radial nodes, one particle per second is generated at each node and the data for 10000 bubbles are used in the calculation of time-averaged IAC. The bubbles that do not pass the sensors, and of which part is out of the channel are excluded from calculation. The generated bubbles are assumed to have the velocity given by Peebles et al.[12] and Davis et al.[13]

The theoretical time averaged interfacial area concentration for the surface represented by the Eq. (26) is given by Eq. (27).

$$z = f(x,y) \tag{26}$$

$$\bar{a}_i^t = \frac{1}{\Omega} \sum_j \frac{1}{|\vec{v}_{iz}|} \sqrt{1 + \left(\frac{\partial z}{\partial x}\right)^2 + \left(\frac{\partial z}{\partial y}\right)^2} \tag{27}$$

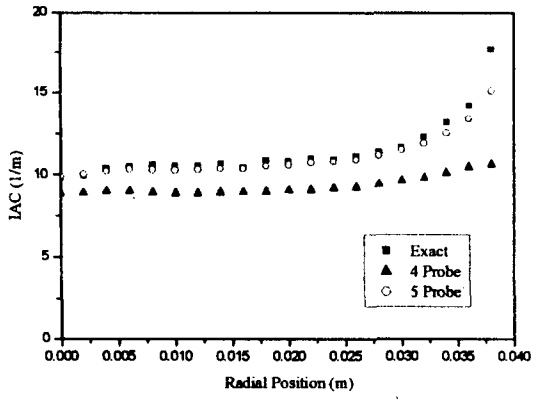

Fig. 10. Total IAC

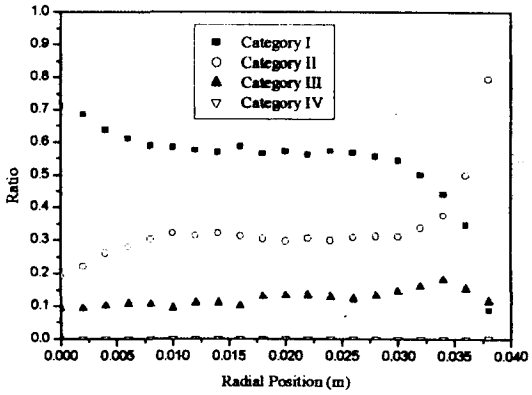

Fig. 11. The Contribution of Each Case to the IAC

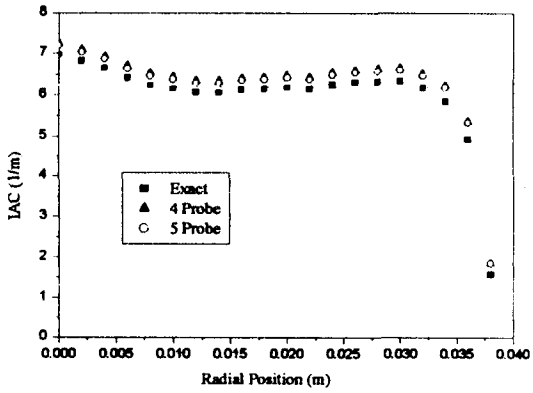

Fig. 12. The IAC for Category I

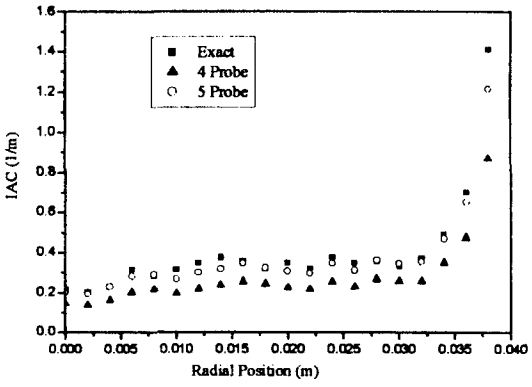

Fig. 13. The IAC for Category II

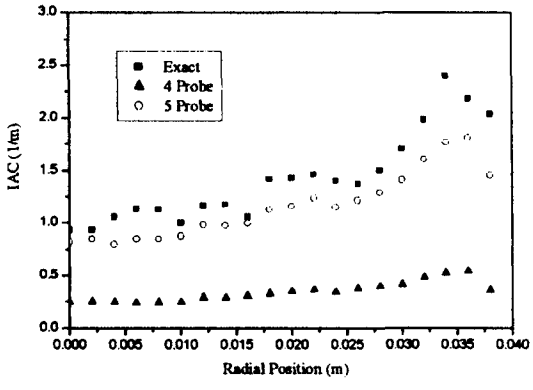

Fig. 14. The IAC for Category III

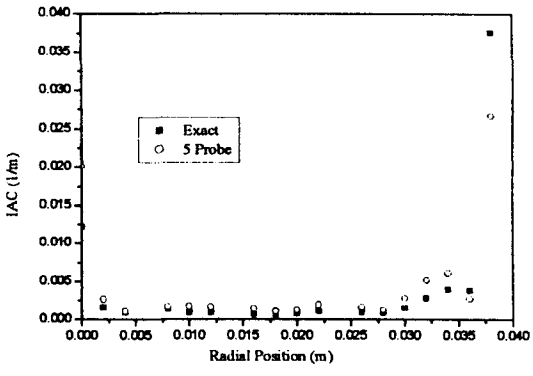

Fig. 15. The IAC for Category IV

An ideal cap bubble has a spherical upper interface and a flat bottom interface. The surface of the sphere that has a radius, r, and of which the center is on the coordinates of (x_0, y_0, z_0) is

represented by Eq. (28) and the flat surface is given by Eq. (29).

$$(x-x_0)^2+(y-y_0)^2+(z-z_0)^2=r^2 \qquad (28)$$

$$z=\text{const} \qquad (29)$$

The theoretical value of the local time-averaged IAC can be obtained analytically from Eqs. (27)~(29).

4. Results and Discussion

Fig. 10 shows the time averaged IAC being compared with that of the four sensor conductivity probe and the theoretical values. On the whole, the five sensor probe method gives satisfactory results, but the four sensor probe method underestimates the IAC. As the probe approaches the wall, some interfaces miss the one or more of the rear sensors, and both of the methods more or less underestimate the interfacial area concentration. This trend indicates that both of the methods underestimate the IAC for the missing bubbles. An independent analysis for the cases that were pre-defined according to the passing type through the sensor were also performed. The contribution of each case to the interfacial area concentration is shown in Fig. 11. As the sensor moves to the wall, the contribution of the missing bubbles increases.

For the case that interface passes all of the sensors (category I), both of the two methods show satisfactory results.(Fig. 12) For the cases that the interface misses one of the symmetric rear sensors (Category II), the estimated values by the five sensor probe agree with the analytical results fairly well.(Fig. 13) The four sensor probe method can estimate the interface area of the upper side of the sphere effectively, but the

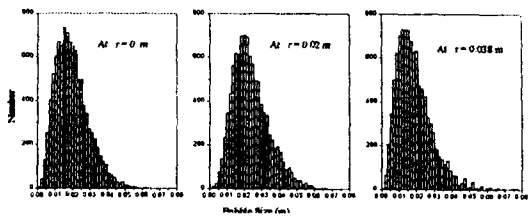

Fig. 16. The Size Distribution of the Sampled Bubble

assumption used to a steep interface is hard to be applied for the flat bottom interface. The four sensor probe method underestimates the IAC by an improper consideration for the bottom interface, whereas the five sensor probe method can treat upper and bottom interfaces effectively by using the information from the central rear sensor. For category III, this trend is more remarkable. (Fig. 14) Category IV can be neglected because the contribution is quite low as shown in Figs. 10 and 15. In Fig. 16, the size distribution used in the simulation is presented at the three radial points.

5. Conclusions

A five sensor probe method to measure the interfacial area concentration (IAC) is developed in this study. The IAC can be obtained by measuring the three components of the velocity vector at a local measuring point and the time delay of the signals from the rear sensors. By using the five sensor probe, one can additionally obtain an axial velocity component from the signal of the central rear sensor. Thus, the four velocity components of the interface at the measuring point can be obtained and one can consider the three sub-cells in the triangular measuring area to get the IAC. The IAC at the measuring point is obtained by averaging that of each sub-cell. This process can reduce the measuring area given by the finite size of the probe, and this aspect also reduces the

curvature effect of the interface for the given size of the probe.

Since the five sensor probe method can treat the upper and bottom sides of an interface pertinently for the missing bubbles, a more systematic approach for the interfaces can be made than the four sensor probe method.

To verify the proposed method, a numerical simulation for cap bubbles generated by a random number generator was carried out. As a result of the numerical simulation, the five sensor probe method is satisfactory for any pre-defined case compared with the four sensor probe method and the analytical results. This study focuses on the validation of the new method using a five sensor probe. Although the shape and size of the bubbles in actual flow can be different from those used in the simulation, and other uncertainties may happen in actual conditions, the five sensor probe method would predict the IAC more exactly than the four sensor probe method for a given measuring area.

Nomenclature

a_i	interfacial area concentration
$\bar{a}_i^t$	time-averaged interfacial area concentration
A	determinant
f_j	function representing the j-th interface
l_d	distance between two of the rear sensors
l_{dk}	length scale that is occupied by a bubble in cell k
$\vec{n}_{sk}$	unit vector in the direction of the k sensor
s_p	projected area of the probe in the flow direction
s_{pk}	projected area that is occupied by a bubble in the cell k
Δs	distance between tips the of two sensors
t	time
Δt_{kj}	transit time for the j-th interface to pass between the front and rear sensor k
v	velocity
x,y,z	coordinates
$\Delta z_{kk'}$	elevation difference of the surface at the position of the k and k' sensors
α_k	angle of sub-cell k on central sensor
α_0	maximum angle between v_{ij} and the mean flow direction vector
ϕ_j	angle between $\vec{v}_{ij}$ and $\vec{n}_j$
η	angle between $\vec{n}_s$ and $\vec{n}_j$
τ	reciprocal of number of interfaces passing a point per unit time
τ_b	bubble residence time
Ω	total measuring time

Subscripts

b	bubble
i	interface
j	interface number
k	rear sensor number
z	z-direction
0	reference

Superscript

t	time-average

References

1. M. Ishii, Thermo-fluid Dynamic Theory of Two-Phase Flow, Eyrolles, Paris, Scientific and Medical Publication of France, New York (1975).
2. I. Kataoka, M. Ishii, and A. Serizawa, "Local Formulation of Interfacial Area Concentration", *Int. J. Multiphase Flow*, **12**, 505 (1986).
3. S. T. Revankar and M. Ishii, "Local Interfacial Area Measurement in Bubbly Flow", *Int. J. Heat Mass Transfer*, **35**, 4, 913 (1992).
4. I. Kataoka and A. Serizawa, "Interfacial Area Concentration in Bubbly Flow", *Nucl. Eng.*

Design, **120**, 163 (1990).

5. G. Kocamustafaogullari, W. D. Huang, and J. Razi, "Measurement and Modeling of Average Void Fraction, Bubble Size and Interfacial Area", Nucl. Eng. Des., 120, 163 (1994).
6. Q. Wu and M. Ishii, "Sensitivity Study on Double-Sensor Conductivity Probe for the Measurement of Interfacial Area Concentration in Bubbly Flow", *Int. J. Multiphase Flow*, **25**, 1, 155 (1999).
7. T. Hibiki, S. Hogsett, and M. Ishii, "Local measurement of interfacial area, interfacial velocity and liquid turbulence in two-phase flow", *Nuc. Eng. and Des.*, **184**, 287 (1998).
8. M. Ishii and S. T. Revankar, Measurement of Interfacial Area Using Four Sensor Probe in Two Phase Flow, DOE/ER/14147, July (1991).
9. M. J. Tan and M. Ishii, Interfacial Area Measurement Methods, ANL-89/5, Feb. (1989).
10. S. T. Revankar, and M. Ishii, "Theory and Measurement of Local Interfacial Area Using a Four Sensor Probe in Two-Phase Flow", *Int. J. Heat Mass Transfer*, **36**, 12, 2997 (1993).
11. G. B. Wallis, One-Dimensional Two-Phase Flow, p. 380, McGraw-Hill, New York, (1969).
12. F. N. Peebles and H. J. Garber, "Studies on the Motión of Gas Bubbles in Liquid", *Chem. Eng. Progr.*, **49**, 88 (1953).
13. R. M. Davis and G. I. Taylor, "The Mechanics of Large Bubbles Rising through Extended Liquids and through Liquids in Tubes", *Proc. Roy. Soc.*, **200**, ser. A, 375, London (1950).

Appendix A. Directional Cosines for the Sensor Tips

- **Sensor 1**

$$x_1 = y_1 = z_1 = 0$$

- **Sensor 2**

$$x_2 = y_2 = 0,\ z_2 = d_{12}$$

- **Sensor 3 (from Fig. A-1, A-2)**

$$x_3 = \sqrt{d_{13}^2 - z_3^2}$$

$$y_3 = 0$$

$$z_3 = \frac{d_{13}^2 + d_{12}^2 - d_{23}^2}{2d_{12}}$$

- **Sensor 4 (from Fig. A-1, A-3)**

$$x_4 = \frac{d_{13}^2 + d_{14}^2 - d_{34}^2 - 2z_3z_4}{2x_3}$$

$$y_4 = \sqrt{d_{14}^2 - x_4^2 - z_4^2}$$

$$z_4 = \frac{d_{12}^2 + d_{14}^2 - d_{24}^2}{2d_{12}}$$

- **Sensor 5 (from Fig. A-1, A-4)**

$$x_5 = \frac{d_{13}^2 + d_{15}^2 - d_{35}^2 - 2z_3z_5}{2x_3}$$

$$y_5 = \sqrt{d_{15}^2 - x_5^2 - z_5^2}$$

$$z_5 = \frac{d_{12}^2 + d_{15}^2 - d_{25}^2}{2d_{12}}$$

- **Directional Cosines**

$(\cos\eta_{x2}, \cos\eta_{y2}, \cos\eta_{z2}) = (0, 0, 1)$

$(\cos\eta_{x3}, \cos\eta_{y3}, \cos\eta_{z3}) = (x_3/d_{13}, 0, z_3/d_{13})$

$(\cos\eta_{x4}, \cos\eta_{y4}, \cos\eta_{z4}) = (x_4/d_{14}, y_4/d_{14}, z_4/d_{14})$

$(\cos\eta_{x5}, \cos\eta_{y5}, \cos\eta_{z5}) = (x_5/d_{15}, y_5/d_{15}, z_5/d_{15})$

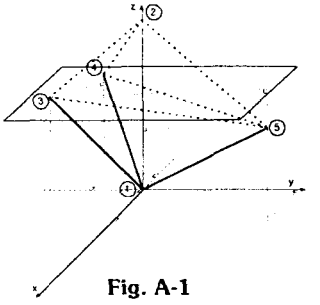

Fig. A-1

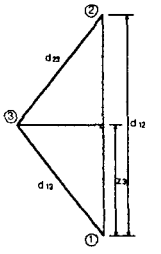

Fig. A-2

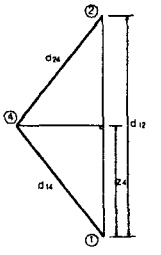

Fig. A-3

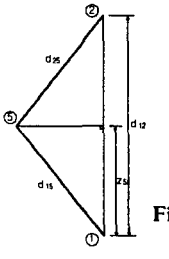

Fig. A-4